Translational and rotational mobility of methanol–d_4 molecules in NaX and NaY zeolite cages: a deuteron NMR investigation

Z. T. Lalowicz [a,*], G. Stoch [a], A. Birczyński [a], M. Punkkinen [b], E. E. Ylinen [b], M. Krzystyniak [c], K. Góra–Marek [d], J. Datka [d],

[a] *H. Niewodniczański Institute of Nuclear Physics of PAN, ul. Radzikowskiego 152, 31–342 Kraków, Poland*

[b] *Wihuri Physical Laboratory, Department of Physics and Astronomy, University of Turku, FI–20014 Turku, Finland*

[c] *The Nottingham Trent University, School of Science and Technology, Clifton Lane, Nottingham, NG11 8NS, United Kingdom*

[d] *Faculty of Chemistry, Jagellonian University, 30–060 Kraków, Poland*

Abstract

Nuclear magnetic resonance (NMR) provides means to investigate molecular dynamics at every state of matter. Features characteristic for the gas phase, liquid–like layers and immobilized methanol–d_4 molecules in NaX and NaY zeolites were observed in the temperature range from 300 K down to 20 K. The NMR spectra at low temperature are consistent with the model in which molecules are bonded at two positions: horizontal (methanol oxygen bonded to sodium cation) and vertical (hydrogen bonding of hydroxyl deuteron to zeolite framework oxygen). Narrow lines were observed at high temperature indicating an isotropic reorientation of a fraction of molecules. Deuteron spin–lattice relaxation gives evidence for the formation of trimers, based on observation of different relaxation rates for methyl and hydroxyl deuterons undergoing isotropic reorientation. Internal rotation of methyl groups and fixed positions of hydrogen bonded hydroxyl deuterons in methyl trimers provide relaxation rates observed experimentally. A change in the slope of the temperature dependence of both relaxation rates indicates a transition from the relaxation dominated by translational motion to prevailing contribution of reorientation. Trimers undergoing isotropic reorientation disintegrate and separate molecules become localized on adsorption centers at 166.7 K and 153.8 K for NaX and NaY, respectively, as indicated by extreme broadening of deuteron NMR spectra. Molecules at vertical position remain localized up to high temperatures. That indicates the dominating role of the hydrogen bonding. Mobility of single molecules was observed for lower loading (86 molecules/uc) in NaX. A direct transition from translation to localization was observed at 190 K.

Key words: deuteron NMR, NMR relaxation, quadrupole coupling, molecular dynamics, methyl group, hydroxyl group, methanol trimers

1 Introduction

Zeolites are used on industrial scale for separation and catalytic transformation of organic molecules. Therefore guest–host interactions have important implications and stimulate investigation in this field [1]. Mobility and bonding of hydrocarbons in zeolites have been studied extensively by numerous methods including studies by deuteron NMR [2–13].

A recent review by Buntkowsky *et al.* [10] provides an excellent introduction to the subject for mesoporous silica materials. The application of NMR methods like diffusometry, proton and deuteron MAS NMR and deuteron solid state NMR allows a step–by–step elucidation of involved interactions along with translational and rotational dynamics of guest molecules [[10] and references therein].

In the present study we focus our attention on methanol in NaX and NaY zeolites. Their framework consists of cubo–octahedral sodalite cages made up of eight 6–membered and 4–membered rings bonded with hexagonal prisms, and have the same structure as natural zeolite, the faujasite. There is a large ellipsoidal super–cage (about 1.18 nm diameter) between cubo–octahedra which is connected with four other super–cages by 12–ring windows with a free aperture of about 0.8 nm. The compositions of typical zeolites NaX and NaY are $Na_{86}[(SiO_2)_{106}(AlO_2)_{86}]$ and $Na_{56}[(SiO_2)_{136}(AlO_2)_{56}]$, respectively. The ratio of Si/Al is equal to 2.4 for zeolite NaY and 1.3 for NaX . Due to the higher density of AlO_4^- tetrahedra in zeolite NaX this framework has bigger negative charge and the framework oxygens are also more negative. The location of cations in zeolites NaX and NaY depends on the cation charge, their degree of hydratation and on the presence of adsorbed molecules. In zeolites NaX and NaY the Na^+ cations are situated inside hexagonal prisms (sites S_I), inside cubo–octahedra (sites $S_{I'}$ and $S_{II'}$) and inside super–cages (sites S_{II} and S_{III}). Only two of them in the super–cage are accessible to adsorbed organic molecules [14–24].

The guest molecules experience different potential depending on the nature and the spatial distribution of the ions and the structural modifications in the

* Corresponding author.
Email address: Zdzislaw.Lalowicz@ifj.edu.pl (Z. T. Lalowicz).

aluminosilicate framework associated with the Si—Al substitution. Accordingly, the diffusive process can be different [25]. The efficiency of migration of guest molecules depends on several factors, *e.g.*, the Si to Al ratio, the nature of the extra framework cations, the presence of sorbed water molecules, the temperature, and the sorbate concentration [26–29]. As reported in the literature, the small polar molecules (such as water, methanol, and ammonia) strongly influence cation distributions [14–18,26–29]. The migration of the cation requires the formation of the complexes which are stable enough to remove the cations from hexagonal prisms [30]. For that reason the partition of the exchangeable cations among the different locations in faujasites is ruled by the type of adsorbed molecules. The interaction of polar molecules with metal cations and the zeolite framework oxygen is vital for the nature of the regent–sorbent (catalyst) bonding [31]. Polar molecules occupy usually certain positions in zeolite. Two basic locations, at cations (called in the following horizontal) and framework oxygens (vertical), of methanol molecules were pointed out [32,33]. With an increasing number of molecules even polymerization is possible. In NaX zeolites the formation of molecular chains is less probable, although there may exist methanol clusters at sodium cations [32].

Structure of methanol trimers $(CH_3OH)_3$ was studied using *ab initio* and density functional methods [34,35]. Their existence as stable structure was evidenced by infrared spectroscopy detecting O—H ring vibrations [36,37]. The structure of methanol trimer is shown in Fig. 1.

The adsorption of methanol is influenced mainly by cations [38]. The preferred position of the methanol is with its oxygen toward the cation S_{II} and the hydroxyl hydrogen pointing toward the framework oxygen [39]. Two methanol molecules adsorbed at two adjacent S_{III}—Na^+ ions may block 12–MR window [40]. However, the most stable structure with the methanol hydroxyl group hydrogen–bonded to the lattice oxygen O_1 in the vicinity of S_{II} cation in faujasite structure was derived from a theoretical analysis of adsorption energy for one methanol molecule [41]. This position, which is illustrated in Fig. 2, will hereinafter be referred to as horizontal, or alternatively I.

The process of the adsorption of methanol over Na^+ exchanged zeolites (ZSM5, MOR, and FAU) was also studied by *in situ* IR spectroscopy. Rep *et al.* [33] reported that the increasing polarity of the zeolite lattice (lower Si/Al) strengthens the interaction between methanol hydrogen atoms, *i.e.*, the hydroxyl as well as methyl hydrogen atoms, and the oxygen atoms of the zeolite framework. The most important interaction takes place between the electron donor lone–pair of the oxygen atoms of methanol and the Na^+ cation. Three types of methanol adsorption states (depending on the Si/Al ratio) in the zeolite pores were distinguished [33]. In the present context the most interesting structure is the adsorption complex which requires the presence of the highest density of

tetrahedral AlO_4^- as *e.g.* in NaX [32]. This state corresponds to the so–called vertical position, alternatively denoted II, which is described by Fig. 3. The higher density of the adsorption sites makes the additional hydrogen bonding between sorbed methanol molecules possible.

The present work was motivated by the deuteron NMR relaxation studies of D_2 in NaY [11] and CD_4 in HY, NaA and NaMordenite [12,42] in which the transition phenomenon between diffusive motion governed by translation to a rotation driven diffusion rates was observed for the first time. The experiments on D_2 in NaY revealed a sharp transition in the deuteron relaxation rate at $T_{RT} = 111\,\mathrm{K}$ from *the low–temperature slope* above T_{RT} to *the high–temperature slope* below T_{RT}. The correlation time of the low–temperature slope just below 111 K amounted to $10^{-7}\,\mathrm{s}$, while that of the high–temperature slope just above 111 K amounted to $10^{-10}\,\mathrm{s}$. At the transition temperature the molecular mobility changed from a mobility characteristic for a condensed gas phase to that representing a liquid–like layer. The transition took place for CD_4 in NaA, NaY and NaMordenite at about 200 K [12,42]. All data indicated a very weak interaction of D_2 and CD_4 molecules with the zeolite framework.

The present study employs deuteron spin–lattice relaxation to provide a further insight into diverse mobility of methanol molecules confined in nanoscale cages at high temperature. Differences in results obtained for NaX and NaY indicate a potential for characterization of binding strengths at various adsorption sites. Structure and nature of interactions can be characterized for molecules localized at various positions on cage walls at lower temperatures. Furthermore, distinct molecular mobilities may be attributed to molecules localized at two different positions, horizontal and vertical.

2 Theoretical background

Deuteron NMR is particularly suitable for the investigation of molecular mobility for a number of reasons. Firstly, the quadrupole coupling constant is two orders of magnitude larger than the dipole–dipole coupling constant for protons. Secondly, the value of the quadrupole coupling constant depends on deuteron location and may provide information on the local structure and bonding. Thirdly and most importantly, since the quadrupole coupling involves only one spin, information on molecular reorientation is not affected by the presence of neighboring nuclei. Therefore, motional averaging of the quadrupole interaction allows the clear discrimination between possible motional models [43].

Molecular reorientations rendering the quadrupole interaction time–dependent and inducing transitions between nuclear Zeeman levels drive the deuteron

NMR relaxation. The spin–spin and spin–lattice relaxation rate constants are given as different linear combinations of spectral density functions weighted by the coefficient A which depends on the square of the quadrupolar coupling constant $\omega_Q = 2\pi C_Q = e^2qQ/\hbar$. In the simplest case of isotropic diffusion characterised by exponential autocorrelation function with a single correlation time τ_c, the spin–lattice relaxation rate constant is given by [44]:

$$\frac{1}{T_1} = A\left[J(\tau_c, \omega_0) + 4J(\tau_c, 2\omega_0)\right], \tag{1}$$

where $J(\tau_c, \omega_0) = \tau_c/(1 + \tau_c^2\omega_0^2)$ is the spectral density function, being the Fourier transform of the autocorrelation function, with $\omega_0/2\pi$ equal to the Larmor frequency. The correlation time τ_c is assumed to follow the Arrhenius formula $\tau_c = \tau_0 \exp(E_a/kT)$ with the activation energy E_a. The temperature dependence of the relaxation rate has an inverted V shape with the maximum at temperature fulfilling the condition $\omega_0\tau_c = 0.616$ which leads to

$$\left(\frac{1}{T_1}\right)_{max} = 1.425\frac{A}{\omega_0}. \tag{2}$$

Fast motions, obeying $\omega_0\tau_c \ll 1$, contribute to the high temperature side of the maximum, while the low temperature side represents the relation $\omega_0\tau_c \gg 1$. The slopes, in some cases unequal, provide the value of the activation energy E_a. Moreover, the value of τ_0 and C_Q can be calculated from the known position of the maximum and its absolute value.

For polycrystalline samples containing methyl groups the effective, motionally averaged value of the parameter A, determining the deuteron spin–lattice relaxation rate constants in Eqs. (1) and (2), depends on the specific character of the motion of the methyl group. If, by isotropic reorientation of the methyl groups the quadrupole interaction becomes completely time–dependent, then for a powder sample $A = 3\omega_Q^2/40$ (see Eq. (17) in [45]). In case when rotation about the methyl symmetry axis is the only motion, then $A = \omega_Q^2/15$. In case when the rotation about the methyl symmetry axis is so fast that $\omega_0\tau_c \ll 1$ the quadrupole coupling constant C_Q is reduced to the fraction 1/3 of its motionsless value according to the relation $C'_Q = (1/2)C_Q(3\cos^2\Theta - 1)$, where Θ is the angle between the symmetry axis and the C—D direction of the electric field gradient. For a methyl group involved in an additional motion (for example if the threefold rotation axis moves on a cone with the opening angle equal to Θ') the same relation may be used [46]. The isotropic reorientation determines the relaxation rate for the fast reorienting methyl groups, and $A = \omega_Q^2/120$ for a powder sample.

The quadrupole coupling constant C_Q for the methyl group CD_3 can adopt slightly different values depending on the local electronic structure of a given

molecular system. In aspirin single crystals C_Q equals 160 kHz [47] and 172 kHz [48]. Analysis of spectra for CD_3CH_2OH in nematic solvents provides C_Q = 180.7 kHz [49]. The value of C_Q has important consequences for the shape of the deuteron NMR spectra. The immobile deuteron Pake doublet, with a peak separation equal $(3/4)C_Q$, characteristic for deuterons in a powder sample, requires correlation times longer than that corresponding to the line narrowing condition, *i.e.* longer than $\tau_c = (4/3)\omega_Q^{-1} = 1.3 \cdot 10^{-6}$ s for methyl groups with $\omega_Q/2\pi = C_Q = 160$ kHz.

3 Experimental

Zeolites NaX (supplied by Sigma–Aldrich) and NaY (purchased from Linde company) were activated *in situ* in an NMR cell. First, samples were evacuated at room temperature for 30 min, then temperature was raised with the rate 5 K/min up to 700 K and kept at this temperature at vacuum for 1 h. The methanol–d_4, (CD_3OD of $HDO + D_2O < 0.03\%$, 99.80% D supplied by EURISO–TOP) was used. The doses of CD_3OD were sorbed in zeolites NaX and NaY up to 100% and 200%, of the total coverage of Na^+ ions. The samples were sealed in 24 mm long glass tubes with the outside diameter 5 mm.

The NMR experiments were carried out over a range of temperatures regulated by the Oxford Instruments CT503 Temperature Controller to the accuracy of ± 0.1 K. The static magnetic field 7 T was created by the superconducting magnet made by Magnex, and the ^2H resonance frequency was equal to 46 MHz. The NMR probe was mounted inside the Oxford Instruments CF1200 Continuous Flow Cryostat. Pulse formation and data acquisition were provided by Tecmag Apollo 500 NMR console. The dwell time was set to 2 μs. The $\pi/2$ pulse equal to 3 μs assured the uniform excitation [50] for our 200 kHz spectra.

NMR spectra were obtained by the Fourier Transformation of the Free Induction Decay (FID) or Quadrupole Echo (QE) signal. For the FID and QE spectra the sequences $(\pi/2)_x$—t and $(\pi/2)_x$—τ—$(\pi/2)_y$—t were used with separation time τ of the order of 50 μs in the QE sequence. The pulse separation time τ was adjusted by means of the home–designed code for Tecmag console in order to optimize QE signal intensity for each temperature. The phase cycling sequence was applied and focused on the FID signal cancellation in the overall signal after the quadrupole echo sequence.

Master spectra were calculated In order to characterise the motion of methanol deuterons for each characteristic mode of motion (*e.g.* for rigid and rotating deuterons of methyl groups) and their combinations were fitted to the recorded deuteron NMR spectra (for details of the method see [13]). The fitting procedure involved adjusting the value of the quadrupole coupling constant and

the width of the Gaussian broadening for all necessary components and led to the evaluation of the corresponding spectral contributions. The Gaussian component was defined by

$$G(\nu) = \frac{1}{\sigma\sqrt{2\pi}} \exp\left[-\frac{(\nu-\nu_0)^2}{2\sigma^2}\right] \tag{3}$$

with the full width at half the maximum (FWHM) equal to $2(2\ln 2)^{1/2}\sigma$, which can be approximated as FWHM $\approx 2.355\sigma$.

For the relaxation time measurements the saturation recovery quadrupole echo pulse sequence: $[(\pi/2)_x\text{—}\tau_n]^n\text{—}\tau_{var}\text{—}(\pi/2)_x\text{—}\tau\text{—}(\pi/2)_y\text{—}t$ and the standard saturation recovery pulse sequence: $[(\pi/2)_x\text{—}\tau_n]^n\text{—}\tau_{var}\text{—}(\pi/2)_x$ were used. The relaxation measurements yielded a set of signal amplitudes which directly led to the magnetization recovery curve $M(\tau_{var})$. The amplitudes were quantified by signal integration over a range in the vicinity of the first FID point beyond the receiver dead time. Alternatively, the QE amplitudes at the maximum were recorded. In the case of be–exponential relaxation the magnetization recovery was fitted by the following formula

$$M(t) = M'\left[1-\exp\left(-\frac{t}{T_1'}\right)\right] + M''\left[1-\exp\left(-\frac{t}{T_1''}\right)\right] + c_0, \tag{4}$$

where $M'+M''+c_0$ is equal to the equilibrium magnetization M_∞. The small positive parameter c_0 takes into account that the saturation may not always be perfect. In the case of exponential magnetization recovery the second term containing M'' was ignored.

The FID and QE sequences were applied according to the complexity of the recored NMR signal. The signals obtained for our samples exhibited a dominating narrow line in the high temperature regime and a broad component for lower temperatures, where too short FID prevents the use of this method. Therefore, both FID and QE sequences are complementary in our measurements in order to provide efficient data acquisition for each regime. In what follows, the temperature T_S will be used to indicate the limit of the FID method for the measurement of the relaxation rate constants. A modification of the subtraction technique introduced by Speier was used [51] to eliminate spurious ringing observed at low temperatures from the NMR probe as well as artefacts at the beginning of the signal at higher temperatures. For eliminating spectral baseline distortion of Fourier–transformed FID signals an extension [52] of Heuers method [53] dedicated to wide ^{2}H NMR spectra was used. The nature of the quadrupole interaction allows to expect symmetric spectra. Thus, the zeroing of the "imaginary" signal in the time domain was possible. An acceptable S/N ratio in the spectra was achieved by signal accumulation.

4 Results and discussion

The figure of merit for the presented analysis of deuteron spin–lattice relaxation of methanol–d_4 in NaX and NaY is the translation to reorientation transition. The transition was observed for the first time for D_2 [11] and CD_4 [12] confined in zeolite cages in the form of an unusual temperature dependence of the spin–lattice relaxation rate constant of deuterons. A radical change in the relaxation rate $1/T_1$ was observed at a transition temperature T_{TR}, from a low temperature slope $1/T_1 \sim 1/\tau_c$ ($\omega_0\tau_c \gg 1$, $T > T_{TR}$) to a high temperature slope of $1/T_1 \sim \tau_c$ ($\omega_0\tau_c \ll 1$, $T < T_{TR}$). The two motional regimes, discerned from the relaxation data, mapped onto two distinct dynamical behaviours below and above the transition temperature. Above the transition temperature molecules have translational freedom in zeolite cages. Molecules, scattering off zeolite walls and other molecules, change their orientation in space by only a small angle at each collision. Therefore many such collisions are needed to provide reorientation efficient in relaxation and the effective correlation time is long. Below the transition temperature molecules roll over cage walls. Rotation provides an efficient relaxation mechanism and the effective correlation time is shortened by three orders of magnitude [11].

4.1 Relaxation above T_S for methanol–d_4 in NaX and NaY

The temperature dependence of the deuteron relaxation rate for methanol–d_4 (172 molecules per unit cell) in NaX zeolite is shown in Fig. 4. The recorded magnetization recovery above T_S was fitted with a bi–exponential function according to Eq. (4). Isotropic reorientation has to be considered as spectra are narrow in this range. Both relaxation rates exhibit a similar temperature dependence, but there is about one order of magnitude difference between them. Based on the weights of the respective relaxation rates we may attribute the faster relaxation rate to OD groups (Fig. 6). The slower rate for CD_3 groups is a consequence of the reduction by 1/3 of the quadrupole coupling constant due to fast internal rotation about the threefold symmetry axis. This means that the methyl deuterons relax *via* isotropic reorientations, and therefore the multiplier A in Eqs. (1) and (2) equals $\omega_Q^2/120$. Hydroxyl deuterons undergo isotropic reorientation for which $A = 3\omega_Q^2/40$. It is worth noting that the ratio of experimentally observed relaxation rate constants is close to 9 (C_Q for deuterons in O—D is usually larger than for methyl groups [54–56]).

Relaxation data indicate that we have to consider a set of methanol molecules undergoing isotropic reorientation with internally fast rotating methyl groups and immobile OD groups. Single molecules can be excluded, as it will be shown below, as in this case also OD groups perform rotation.The above relaxation

results can be explained by considering some degree of clustering of methanol molecules. Two mechanisms are in order here. Firstly, a chain of molecules may be formed by hydrogen bonds of hydroxyl deuteron and oxygen in neighboring methanol molecules [32,33]. Secondly, a formation of methanol trimers with OD groups at positions fixed inside them is possible [38,37]. Trimers form a stable, closed symmetric structure for which reorientation is possible [34]. The picture of the diffusive motion of methyl trimers may be more complex. Similarly to benzene molecules in zeolites [7,8], methyl trimers may in principle rotate about an axis perpendicular to their plane. Such rotation averages the deuteron quadrupole interaction of methyl and OD groups by the factor of one half. This rotation as an exclusive motion can be ruled out in our case taking into account the observed spectra and relaxation rates. Thus, translation and more isotropic reorientation of methyl trimers must be the dominating mechanism behind the deuteron spin lattice relaxation in NaX zeolite above T_S. However, as it will be shown below, that observation refers to a fraction of molecules as spectra of remaining molecules at position II are broad.

The overall picture of methanol molecular dynamics emerging from the analysis of the deuteron relaxation data in NaX zeolite seems to be similar in the case of NaY zeolite with 112 molecules per unit cell (see Fig. 5). However, the transition from the relaxation dominated by translational diffusion to prevailing rotation contribution appears at different temperatures, higher for OD (T^1_{TR}) than for CD_3 (T^2_{TR}) (Figs. 4 and 5, Table 1). Activation energies are similar for both groups (Table 1). Therefore the slopes in temperature dependence of the relaxation rates are expected to be parallel. Under these conditions transitions should appear at the same temperature for both groups. Experimental results show that $T^1_{TR} > T^2_{TR}$, and the transition appears in a wider range of temperature for CD_3 groups. It may result from intermolecular interactions at collisions, making them effective down to lower temperature for CD_3. Different T^n_{TR} values for NaX and NaY zeolites may indicate on influence of bonding to framework oxygen, even at collisions, which is affecting the mobility of the methyl groups of trimers. That shows in microscopic scale the effect of surface mediated diffusion [57]. The bonding of CD_3 deuterons to framework oxygen atoms is weaker in NaY and thus temperatures T^n_{TR} are lower than in NaX.

As mentioned before, methanol molecules can be bonded either to sodium cations (*via* free electron pair of oxygen) or to framework oxygens (*via* hydrogen bonding O—D$\cdots$O). The electrical charge on sodium cations is partially neutralized by framework oxygen atoms. The extent of neutralization of Na^+ is smaller in NaY and the electrical charge of Na^+ is higher [58]. Therefore the interaction of the negative charge of methanol oxygen with the more positive charge of Na^+ in NaY is stronger than in NaX. This observation, however, is in disagreement with the lower temperature T_S of immobilization of methanol in NaY deduced from the relaxation data.

Another kind of interaction of methanol with zeolite is the hydrogen bonding of O—D with framework oxygen atoms. In the zeolite NaY the framework oxygen atoms are less negative than in NaX (due to smaller number of AlO_4^- tetrahedra). The hydrogen bonding is weaker which agrees well with lower T_S. The fact that the results give evidence for a weaker interaction of methanol with the zeolite framework in NaY suggests that the hydrogen bonding of methanol with framework oxygen atoms plays more important role in faujasites than interaction with Na^+cations.

The weights of the two rate constants describing deuteron spin–lattice relaxation of methanol–d_4 caged in NaX and NaY are shown in Fig. 6. The weight attributed to OD groups is reduced to 0.175 ± 0.03 from the theoretical value of 0.25 (the theoretical value for the weight attributed to CD_3 groups is 0.75). The reduction of weights may indicate that contribution of some CD_3 and OD groups was not detected using FID. Spectrum obtained using QE sequence at 175 K (Fig. 7) shows a narrow line on the background of the doublet of rotating CD_3 groups and Pake doublet of immobile OD. More about broad components in the next chapter. The narrow and broad components can be attributed to two subsystems of molecules with different mobility. The broad components are related to hydrogen bonded methanol at vertical position II (more in Chapter 4.3). Their contribution decays on thermally activated way due to increasing amplitude of motions and collisions with free to diffuse other molecules. Narrow line represents molecules coupled into trimers, performing isotropic reorientation and translation, with a contribution decreasing on temperature approaching T_S. No exchange between the subsystems was detected at 175 K in deuteron 2D spectra [59].

Solid echo based relaxation measurements were extended to temperatures just above T_S following the conclusion above and in order to complete the analysis of the deuteron spin–lattice relaxation data. Here rate constants obtained from FID were not detected. Selective measurements of relaxation rates from recovery of separate spectral components: narrow line, CD_3 doublet and Pake doublet, confirm the assignement of relaxation rates. This proves that reorienting and localized molecules coexist in a range of temperature above T_S. Three relaxation rate constants had to be used to describe the magnetization recovery sufficiently accurately just above and below T_S. These effects resulting from a wide distribution of correlation times will be presented in detail elsewhere.

The following scenario, may be proposed at the molecular level, based on the experimental evidence from the analysis of the deuteron spin lattice relaxation data. Methanol trimers, moving more slowly on cage walls when temperature approaches T_S, may break and single methanol molecules form hydrogen bonds preferentially to the framework oxygen atoms (structure II). Then some methanol molecules may be attracted by framework cations nearby and form

the horizontal structure I.

4.2 Spectra of methanol–d_4 in NaX below T_S

Spectra of methanol–d_4 in NaX in the temperature range from 20 K to 160 K are shown in Figs. 8 and 9. Spectrum at 20 K was fitted consistenly by four Pake doublets with contributions 7%, 22%, 17% and 17%, and quadrupole coupling constants 152, 175, 205 and 232 kHz, respectively. In addition to Pake doublets, there are also two doublets attributed to rotating methyl groups, contributing 17% and 2%, with $C_Q = 150$ kHz and 120 kHz, respectively.

Upon temperature increase above 30 K the contributions of individual spectral components start to change (Fig. 10). The total contribution of Pake doublets decreases to reach a *plateau* value of 12% at 133K and the contribution from the rotating methyl groups increases to 55%. The contribution of the Gaussian component increases to the maximum value 34% at *ca.* 70 K. The parameter σ of this Gaussian component changes from 13.5 kHz at 20 K to 10.5 kHz at 160 K. The contribution of the doublet representing rotating methyl groups with $C_Q = 120$ kHz is growing with increasing temperature at the expense of the Gaussian component.

4.3 Methanol mobility at two locations below T_S

As the starting point for the assignment of spectral components we assume that the horizontal (Fig. 2) and vertical locations (Fig. 3) of methanol molecules are equally populated. We label them CD_3OD(I) and CD_3OD(II), respectively. The deuterons of methyl groups and hydroxyl groups in either position contribute 37.5% and 12.5%, respectively. Methyl CD_3(I) and OD(I) groups belong to the methanol molecules localized at sodium cations and may be bonded to framework oxygens, what restricts their mobility. Methyl groups CD_3(II) are expected to have lower activation energy for uniaxial rotation. OD(II) is involved in a strong hydrogen bonding to the framework oxygen. A methyl molecule at a vertical position is shown in Fig. 3 at the orientation corresponding to the minimum moment of inertia about an axis along the O$\cdots$D hydrogen bond. Rotation of the whole molecule about that axis is possible. The threefold symmetry axis of methyl group makes the angle of 22.8 degrees with the rotation axis.

The assignment of spectral components is presented in Table 2. Spectra below 30 K are temperature independent. The contribution of CD_3(II) is distributed among the threefold rotation doublet and Gaussian components (Table 2). As for an explanation we assume that all CD_3(II) perform fast rotation about the

threefold symmetry axis, however for some of them the axis undergoes chaotic motion in limited space which smears out the doublet into the Gaussian component. All other deuterons contribute to the four Pake doublets mentioned above. These doublets are attributed to immobile deuterons in CD_3OD(I) and OD(II). More precise assignement will be possible with a stepwise onset of mobility at higher temperatures.

All CD_3(I) perform threefold rotation ($C_Q = 150\,\mathrm{kHz}$) and all CD_3(II) contribute to the Gaussian at about 50 K. All OD(I) and OD(II) remain rigid. From about 70 K upwords a contribution to the rotation related doublet, attributed to OD(I) groups rotating about a threefold axis, was detected. Thus, above 70 K only OD(II) contribute to the Pake doublet, however with two components characterized by the quadrupole coupling constants 177 kHz and 205 kHz, seen also at 175 K. At about 80 K a second rotational doublet appears with a smaller quadrupole coupling constant $C_Q = 120\,\mathrm{kHz}$. It results from a rotation of the threefold axis of some CD3(II) on a cone with 19 degrees opening angle. Its contribution increases at the expense of the Gaussian component. The above result supports the idea of rotation of methanol molecules at position II about the axis of minimum moment of inertia.

The quadrupole coupling constant obtained from fitting the spectra of the rotating CD_3 groups is lower than observed in crystals [47,48]. Moreover the results indicate a temperature dependence. Namely, C_Q is equal 150 kHz at 20 K, 146 kHz at 100 K and 142 kHz at 285 K. Such stepwise reduction of the quadrupolar coupling constant results from fluctuations of methyl groups CD_3(II) positions even at 20 K.

4.4 NaX with 100% abundance of CD_3OD

The motivation for the measurement of the sample of zeolite NaX with 100% coverage of CD_3OD (about 86 molecules per unit cell) was twofold: to separate different contributions to deuteron NMR spectra, and spin–lattice relaxation. Examples of deuteron NMR spectra of zeolite NaX with 100% coverage of CD_3OD are shown in Fig. 11.

There are three spectral components at 10 K: a Gaussian component (13%, $\sigma = 20\,\mathrm{kHz}$), a component due to threefold axis rotation (51%) and a component due to contributions from rigid molecules (36%). The numerical spectral line decomposition yields five quadrupolar coupling constants for Pake doublets representing immobile deuterons. Previous analysis allows to attribute the Gaussian component to a fraction of CD_3(II). Remaining fraction of 24% of CD_3(II), together with 27% of CD_3(I), contributes to the doublet attributed to rotating methyl deuterons. A fraction of 11% of CD_3(I) contributes to

Pake doublets characterized by C_Q equal to 154 kHz and 177 kHz, as these components disappear above 40 K and contribute to the component due to threefold axis rotation (Figs. 12 and 13).

Spectra are practically temperature independent in the range $60 \div 100$ K (Fig. 13). Dynamics of CD_3(II) remains unchanged and all CD_3(I) groups are rotating. A new component appears above 100 K (Table 3). It is caused by the transfer of spectral intensity from the Pake doublet with $C_Q = 97$ kHz, attributed to OD(I) groups, which is not observed above 100 K (Fig. 12). Thus there is increasing fraction of rotating OD(I) groups ($C_Q = 102$ kHz) which reaches the maximum of $13 \pm 1\%$ at 170 K (Fig 13). Hydrogen bonded OD(II) contribute to the remaining Pake doublets with C_Q equal to 205 kHz and 232 kHz. Threefold rotation component ($C_Q = 135$ kHz) reaches 38% at 185 K. Both values of contributions confirm the assignement to OD(I) and CD_3(I), repectively. The Gaussian and rigid components, 39% and 9%, refer to CD_3(II) and OD(II), respectively. The doublets due to rotating OD(I) groups and CD_3(II) are broadened significantly on increasing temperature and a narrow Gaussian component appears at 185 K indicating increasing isotropic mobility of molecules. Narrow spectra are obtained above $T_S = 190$ K.

Two time constants are observed in the temperature dependence of the spin–lattice relaxation rate above T_S (Fig. 14). The relaxation rate with a maximum at about 285 K was attributed to rotating OD(II) groups as its weight amounts only about 10%. The fit to the maximum yields $C_Q = 150.6$ kHz, $E_a = 20.6$ kJ/mol and $\tau_0 = 4.3 \cdot 10^{-13}$ s. The value and temperature dependence of the second time constant reminds the rate previously attributed to rotating methyl groups in trimers with high translational freedom undergoing isotropic reorientation. Activation energy $E_a = 5.4$ kJ/mol appears to be much smaller than for high loading (Table 1). The activation energy characterizes the relaxation mechanism *via* collisions of single molecules, with fast internal rotations of both CD_3 and OD, performing isotropic reorientation. It refers, as for 200% loading discussed above, to a fraction of molecules as those at vertical position avoid observation with FID. Multiexponential relaxation was observed below T_S using QE. That indicates a broad distribution of correlation times and will be discussed in a paper which follows.

5 Conclusions

Our results provide a picture of the molecular mobility within limits of NMR spectroscopic window. The details of its description evolved with increasing volume of experimental data. Freely moving trimers and hydrogen bonded molecules coexist at high temperature and at high loading. The transition from translation to reorientation may be visualized as a transition from surface–free

to surface mediated diffusion [57]. Methanol trimers diffuse freely in super–cages and then on the cage walls. Their contact with the cage walls leads only to restricted, two–dimensional diffusion below the transition temperature. Reorientation of trimers is stopped at T_S as indicated by extreme broadening of deuteron spectra. The mechanism of the transition at molecular level as well as the way of trimers dissintegration, about which we may now only speculate, will be studied by deuteron 2D spectroscopy.

The low temperature positions of localized molecules were deduced on the basis of sets of CD_3 and OD groups with different mobility related to different local potentials, leading to different spectra. However, it may be considered as a simplification, as the real system is highly non–uniform.

The mobility of the molecules depends on their location at the adsorption centers. Immobile deuterons both from methyl and hydroxyl groups are characterized by different quadrupole coupling constants. This observation indicates an external contribution to the intramolecular electric field gradient, which depends on the location in the framework. Towards this end, a more detailed, theoretical analysis of the quadrupole coupling constants would be highly desirable and work along these lines is in progress.

Acknowledgements

This study was a part of the project generously supported by the National Science Centre, Poland, Grant No. N N202 127939 during 2010–2013.
Finacial support from Jenny and Antti Wihuri Foundation is acknowledged.

References

[1] D.F. Shantz, R.F. Lobo, Top. Catal. **9** (1999) 1.

[2] M.A. Hepp, V. Ramamurthy, D.R. Corbin, C. Dybowski, J. Phys. Chem. **96** (1992) 2629.

[3] A.G. Stepanov, A.A. Shubin, M.V. Luzgin, H. Jobic, A. Tuel, J. Phys. Chem. B **102** (1998) 10860.

[4] A.G. Stepanov, M.M. Alkaev, A.A. Shubin, M.V. Luzgin, T.O. Shegai, H. Jobic, J. Phys. Chem. B **106** (2002) 10120.

[5] S.M. Auerbach, L.M. Bull, N.J. Henson, H.I. Metiu, A.K. Cheetham, J. Phys. Chem. **100** (1996) 5923.

[6] Y.H. Chen, L.P. Hwang, J. Phys. Chem. **103** (1999) 5070.

[7] O. Isfort, B. Bodenberg, F. Fujara, Chem. Phys. Lett. **228** (1998) 71.

[8] O. Isfort, B. Geil, F. Fujara, J. Magn. Reson. **130** (1998) 45.

[9] P. Medick, M. Vogel, E. Rössler, J. Magn. Reson. **159** (2002) 126.

[10] G. Buntkowsky, H. Breitzke, A. Adamczyk, F. Roelofs, T. Emmler, E. Gedat, B. Grünberg, Y. Xu, H.–H. Limbach, I. Shenderovich, A. Vyalikh, G. Findenberg, Phys. Chem. Chem. Phys. **9** (2007) 4843.

[11] J.S. Blicharski, A. Gutsze, A.M. Korzeniowska, Z.T. Lalowicz, Z. Olejniczak, Appl. Magn. Reson. **27** (2004) 183.

[12] A. Birczyński, M. Punkkinen, A.M . Szymocha, Z.T. Lalowicz, J. Chem. Phys. **127** (2007) 204714.

[13] Z.T. Lalowicz, G. Stoch, A. Birczyński, M. Punkkinen, M. Krzystyniak, K. Góra–Marek, J. Datka, Solid State Nucl. Magn. Reson. **37** (2010) 91.

[14] F. Haase, J. Sauer, J. Microporous Mesoporous Mater. **35–36** (2000) 379.

[15] K. Góra–Marek, Vib. Spectrosc. **52** (2010) 31.

[16] F. Gilles, J.L. Blin, C. Mellot–Draznieks, A.K. Cheetham, B.L. Su, Stud. Surf. Sci. Catal. **154 B** (2004) 1757.

[17] P. Norby, F.I. Poshni, A.F. Gualtieri, J.C. Hanson, C.P. Grey, J. Phys. Chem. B **105** (5) (1998) 839.

[18] N.A. Ramsahye, R.G. Bell, J. Phys. Chem. B **109** (2005) 4738.

[19] V. Bosacek, J. Phys. Chem.**97** (1993) 10732.

[20] M. Ziolek, J. Czyzniewska, J. Lamotte, J.C. Lavalley, React. Kinet. Catal. Lett. **53** (1994) 339.

[21] M. Ziolek, J. Czyzniewska, J. Lamotte, J.C. Lavalley, Zeolites **16** (1996) 42.

[22] P. Salvador, W.J. Kladnig, Chem. Soc., Faraday Trans. **73** (1977) 1153.

[23] A. Nicolas, S. Devautour–Vinot, G. Maurin, J.C, Giuntini, F. Henn, J. Phys. Chem. C **111** (2007) 4722.

[24] S.G. Izmailova, I.V. Karetina, S.S. Khvoshchewv, M.A. Shubaeva, Colloid Interface Sci., **165** (1994) 318.

[25] Ph. Grenier, F. Meunier, P.G. Gray, J. Kärger, Z. Xu, D.M. Ruthven, Zeolites **14** (1994) 242.

[26] G. Mirth, J.A. Lercher, M.W. Anderson, J.J. Klinowski, Chem. Soc., Faraday Trans. **86** (1990) 3039.

[27] J. Kotrla, D. Nachtigallova, L. Kubelkova, L. Heeribout, C. Doremieux–Morin, J. Fraissard, J. Phys. Chem. B **102** (1998) 2454.

[28] S.R. Blaszkowski, R.A. Van Santen, J. Phys. Chem. B **101** (1997) 2292.

[29] F. Haase, J. Sauer, J. Am. Chem. Soc. **117** (1995) 3780.

[30] D.F. Plant, G. Maurin, R.G. Bell, J. Phys. Chem. B **110** (2006) 15926.

[31] G. Maurin, D.F. Plant, F. Henn, R.G. Bell, J. Phys. Chem. B **110** (2006) 18447.

[32] M. W. Anderson, P. J. Barrie, J. Klinowski, J. Phys. Chem. **95** (1991) 235.

[33] M. Rep, A.E. Palomares, G. Eder–Mirth, J.G. van Ommen, N. Rosch, J.A. Lercher, J. Phys. Chem. B **104** (2000) 8624.

[34] O. Mó, M. Yáñez, J. Elguero, J. Chem. Phys. **107** (1997) 3592.

[35] U. Buck, J.-G. Siebers, R. J. Wheatley, J. Chem. Phys. **108** (1998) 20.

[36] F. Huisken, M. Kaloudis, M. Koch, O. Werhahn, J. Chem. Phys. **105** (1996) 8965.

[37] R. A. Provencal, J. B. Paul, K. Roth, C. Chapo, R. N. Casaes, R. J. Saykally, G. S. Tschumper, H. F. Schaefer III, J. Chem. Phys. **110** (1999) 4258.

[38] R. Schenkel, A. Jentys, S.F. Parker, J.A. Lercher, J. Phys. Chem. B **108** (2004) 7902.

[39] D.F. Plant, A. Simperler, R.G. Bell, J. Phys. Chem. B **110** (2006) 6170.

[40] T. Nanok, S. Vasenkov, F.J. Keil, S. Fritzsche, Microporous Mesoporous Mater. **127** (2010) 176.

[41] J. Sielk, T. Wieland, A. Lüchow, J. Mol. Structure THEOCHEM **910** (2009) 8.

[42] A. Birczyński, M. Punkkinen, A.M. Szymocha, Z. T. Lalowicz, Stud. Surf. Sci. Catal., Zeolites and Related Materials: Trends, Targets and Challenges **174** (2008) 921.

[43] G. Stoch, E.E. Ylinen, M. Punkkinen, B. Petelenz, A. Birczyński, Solid State Nucl. Magn. Reson. **35** (2009) 180.

[44] A. Abragam, *The Principles of Nuclear Magnetism* (Oxford University Press, Oxford, UK 1961), Chap. VIII.

[45] Z. T. Lalowicz, M. Punkkinen, A.H. Vuorimäki, E.E. Ylinen, A. Detken, and L.P. Ingman, Solid State Nucl. Magn. Reson. **8** (1997) 89.

[46] C.P. Slichter, *Principles of Magnetic Resonance* (Springer–Verlag, New York Berlin Heidelberg, Germany 1996), Chap. 3.

[47] A. Detken, P. Focke, H. Zimmermann, U. Haeberlen, Z. Olejniczak, Z. T. Lalowicz, Z. Naturforsch. **50a**, (1995) 95.

[48] A. Detken, H. Zimmermann, J. Chem. Phys. **108** (1998) 5845.

[49] G.C. Lickfield, A.L. Beyerlein, G.B. Savitsky, L.E. Lewis, J. Phys. Chem. **88** (1984) 3566.

[50] M. Bloom, J.H. Davis, M.I. Valic, Can. J. Phys. **58** (1980) 1510.

[51] P. Speier, G. Prigl, H. Zimmermann, U. Haeberlen, E. Zaborowski, S. Vega, Appl. Magn. Reson. **9** (1995) 81.

[52] G. Stoch, Z. Olejniczak, J. Magn. Reson. **173** (2005) 140.

[53] A. Heuer, U. Haeberlen, J. Magn. Reson. **85** (1989) 79.

[54] H. W. Spiess, B. B. Garret, R. K. Sheline, and S. W. Rabideau, J. Chem. Phys. **51**, 1201 (1969).

[55] M. Scheuermann, B. Geil, F. Löw, and F. Fujara, J. Chem. Phys. **130**, 024506 (2009).

[56] D. Freude, H. Ernst, and I. Wolf, Solid State Nucl. Magn. Reson. **3**, 271 (1994).

[57] D.F. Plant, G. Maurin, R.G. Bell, J. Phys. Chem. B **111** (2007) 2836.

[58] C.L. Angell, P.C. Schaffer, J. Phys. Chem. **70** (1966) 1413.

[59] E. Rößler, B. Pötzchner, private communication.

Table 1

Activation energies and transition temperatures for methanol–d_4 in NaX and NaY zeolites at high temperature.

Zeolite	NaX				NaY			
	E_a(a) [kJ/mol]	E_a(b) [kJ/mol]	T_{TR} [K]	T_S [K]	E_a(a) [kJ/mol]	E_a(b) [kJ/mol]	T_{TR} [K]	T_S [K]
OD	14.2	12.7	245	166.7	13.5	10.0	230	153.8
CD_3	12.9	10.4	232	166.7	14.3	11.3	212.8	153.8

Table 2

Assignment of spectral contributions for 200% CD_3OD in NaX .

Spectral component	175 K	125 K	70 K	50 K	30 ÷ 20 K
rotation (150 kHz)	CD_3OD(I)	CD_3OD(I)	CD_3OD(I)	CD_3(I)	1/2 CD_3(II)
rotation (120 kHz)	1/3 CD_3(II)	1/3 CD_3(II)			
Gaussian	2/3 CD_3(II)	2/3 CD_3(II)	CD_3(II)	CD_3(II)	1/2 CD_3(II)
narrow	isotropic				
rigid	OD (II)	OD (II)	OD (II)	OD (II)	CD_3OD(I)
				+OD(I)	+OD(II)

Table 3

Assignment of spectral contributions for 100% CD_3OD in NaX .

Spectral component	180 K	160 K	60 ÷ 100 K	10 K
rotation (144 kHz)	CD_3(I)	CD_3(I)	CD_3(I) + OD(I)	CD_3(I)
	+CD_3(II)	+CD_3(II)	+CD_3(II)	+CD_3(II)
rotation (102 kHz)	OD (I)	OD (I)	—	—
Gaussian	CD_3(II)	CD_3(II)	CD_3(II)	CD_3(II)
rigid (205 kHz, 232 kHz)	OD (II)	OD (II)	OD (II)	OD (II)
rigid (154 kHz, 177 kHz)	—	—	—	CD_3(I)
rigid (97 kHz)	—	—	OD (I)	OD (I)

Figure captions

Fig.1. Structure of methanol trimer.

Fig.2. Horizontal position of methanol molecule on zeolite faujasite scheleton.

Fig.3. Vertical position of methanol molecule on zeolite faujasite scheleton.

Fig.4. Relaxation rate temperature dependence for 200% CD_3OD in NaX. Symbols $\circ$ and $\Box$ refer to relaxation rates for OD and CD_3, respectively. Values of transition temperatures and activation energies in a and b ranges are given in Table 1. Three time constants on right hand side refer to relaxation of immobilized molecules.

Fig.5. Relaxation rate temperature dependence for 200% CD_3OD in NaY. Other details as in Fig. 3.

Fig.6. Weights of time constants in Figs. 3 and 4. Open and filled symbols refer to methanol in NaX and NaY, while $\circ$ and $\Box$ refer to OD and CD_3, respectively.

Fig.7. Deuteron spectrum of methanol–d_4 (200%) in NaX at 175 K.

Fig.8. Deuteron NMR spectra of 200% CD_3OD confined in NaX at low temperature range: 20 K (a), 38.5 K (b), 50 K (c), 62.5 K (d).

Fig.9. Deuteron NMR spectra of 200% CD_3OD confined in NaX at intermediate temperature range: 90 K (a), 110 K (b), 153 K (c), 160 K (d).

Fig.10. Contributions of spectral components at low and intermediate temperatures (sample as in Figs. 7 and 8). Sum of Pake contributions is depicted with $\blacklozenge$. Contributions of rotating deuterons refer to $\bullet$ and $\circ$ for the quadrupole coupling constant 150 kHz and 120 kHz, respectively. Symbol $\triangle$ is given for the broad Gaussian component.

Fig.11. Deuteron NMR spectra for 100% abundance of CD_3OD in NaX at 10 K (a), 110 K (b), 150 K (c), 185 K (d).

Fig.12. Temperature dependence of Pake doublets contributions (sample as in Fig. 10): C_Q =: 97 kHz ($\blacktriangle$), 154 kHz (+), 177 kHz ($\Box$), 205 kHz ($\diamond$), 232 kHz ($\bigtriangledown$) .

Fig.13. Temperature dependence of contributions of spectral components (sample as in Fig. 10): rotation $C_Q = 102$ kHz ($\bullet$), rotation $C_Q = 144$ kHz ($\circ$), sum of Pake doublets ($\blacklozenge$), broad Gaussian ($\triangle$), narrow Gaussian (+) and ($*$).

Fig.14. Temperature dependence of the relaxation rates (sample as in Fig. 10), $T_S = 190$ K. The marked slope provides $E_a = 5.4$ kJ/mol. Parameters obtained from fitting to the maximum are given in the text.

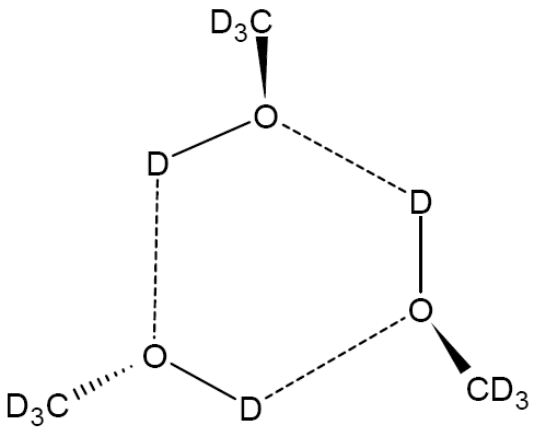

Fig. 1.

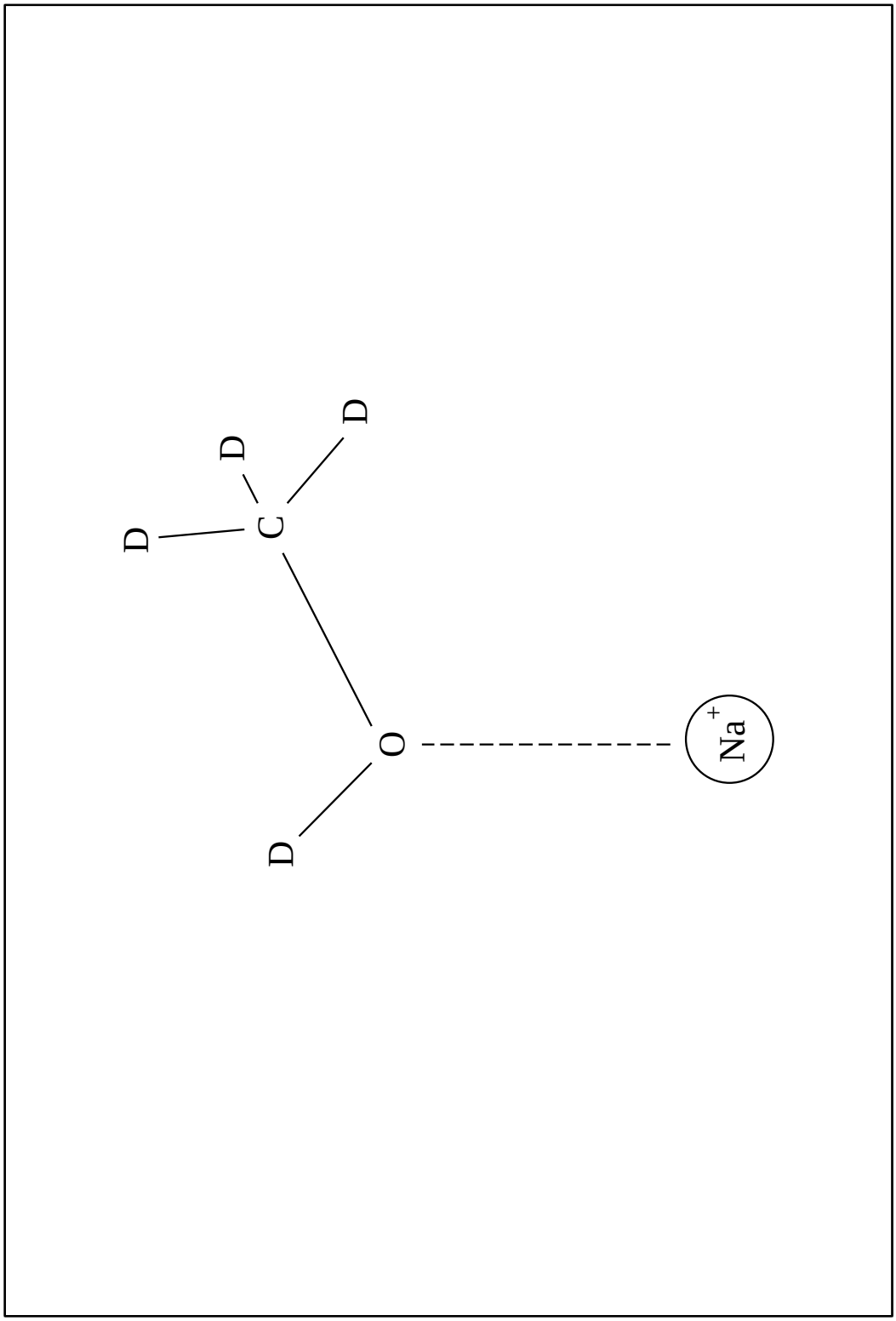

Fig. 2.

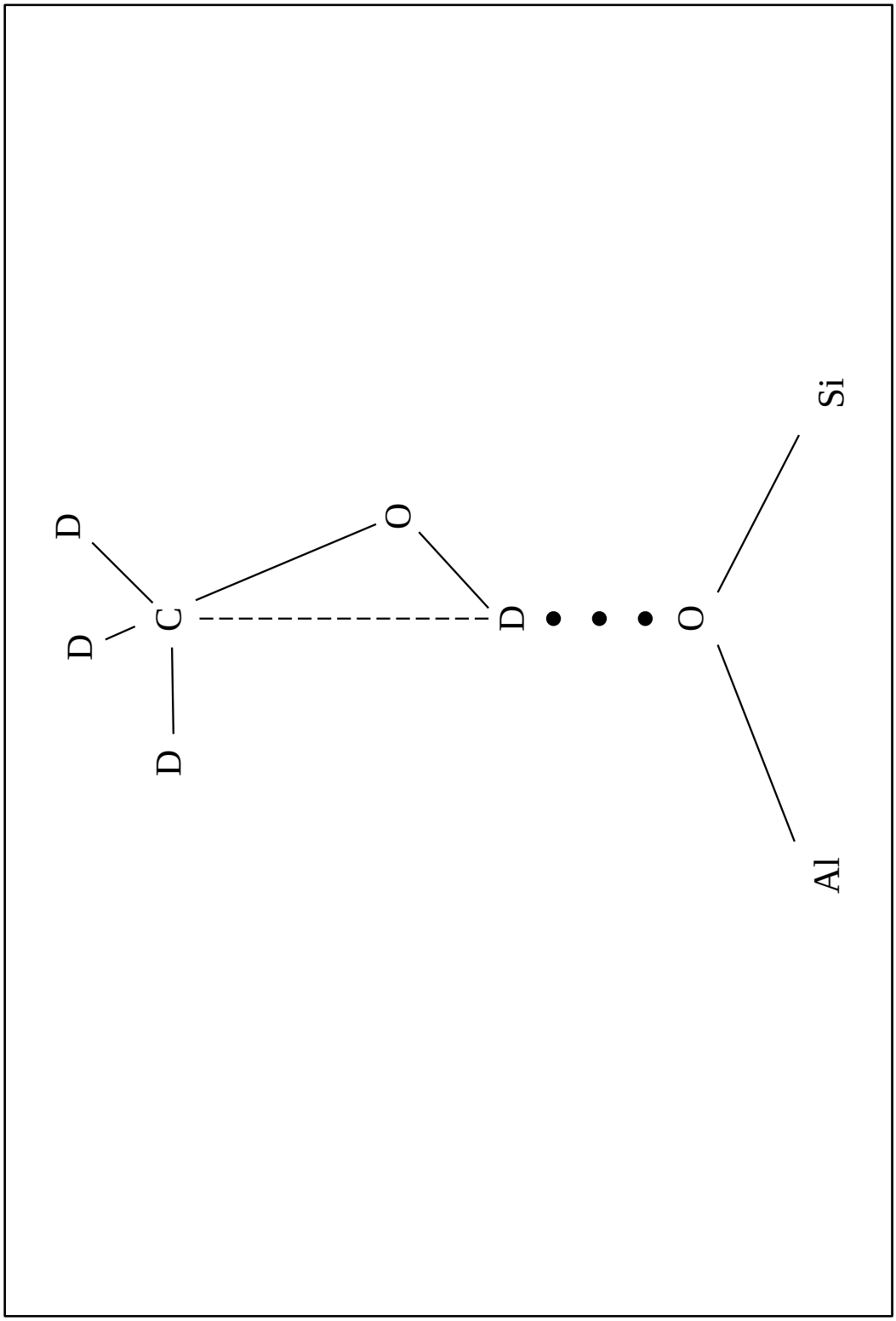

Fig. 3.

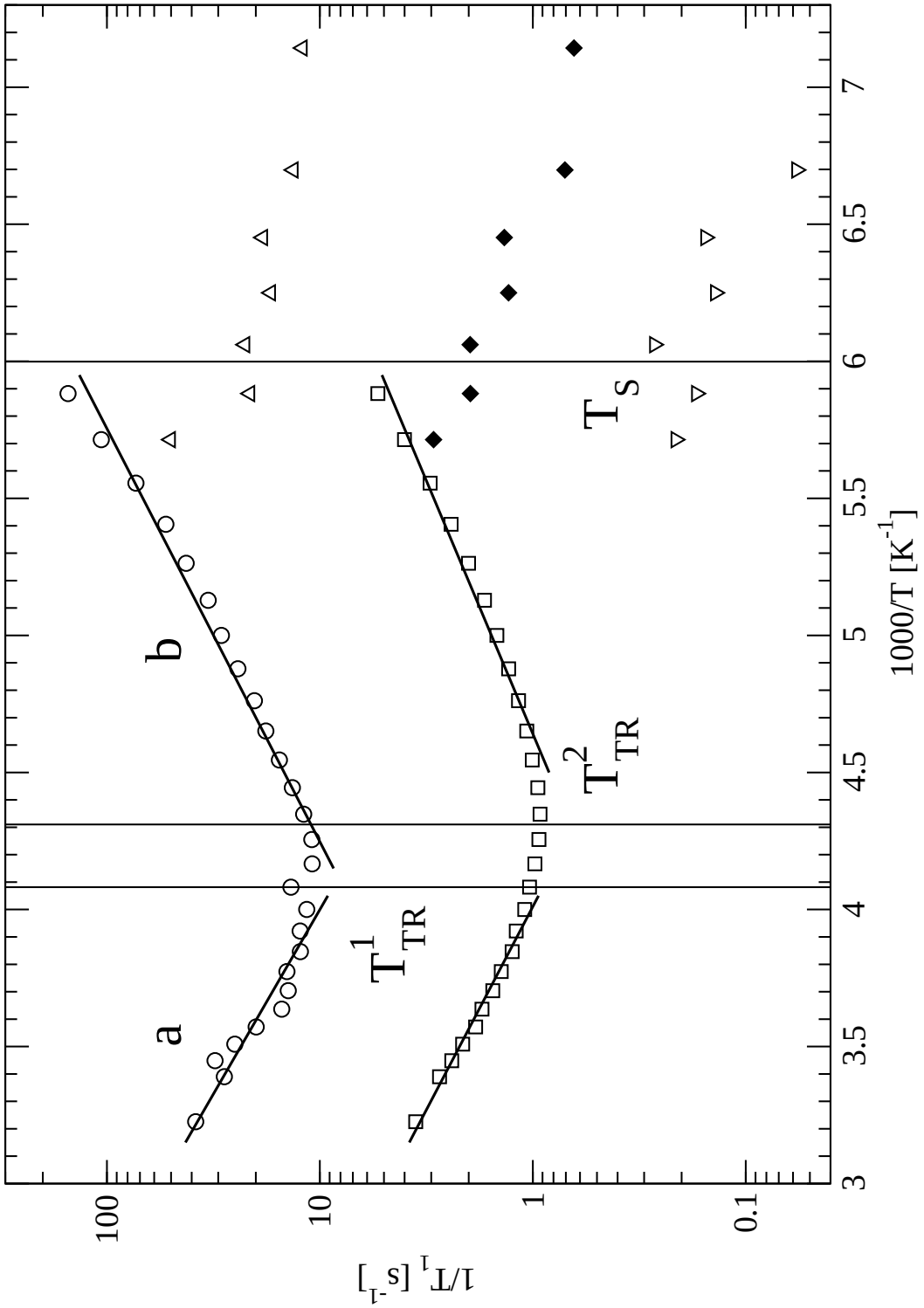

Fig. 4.

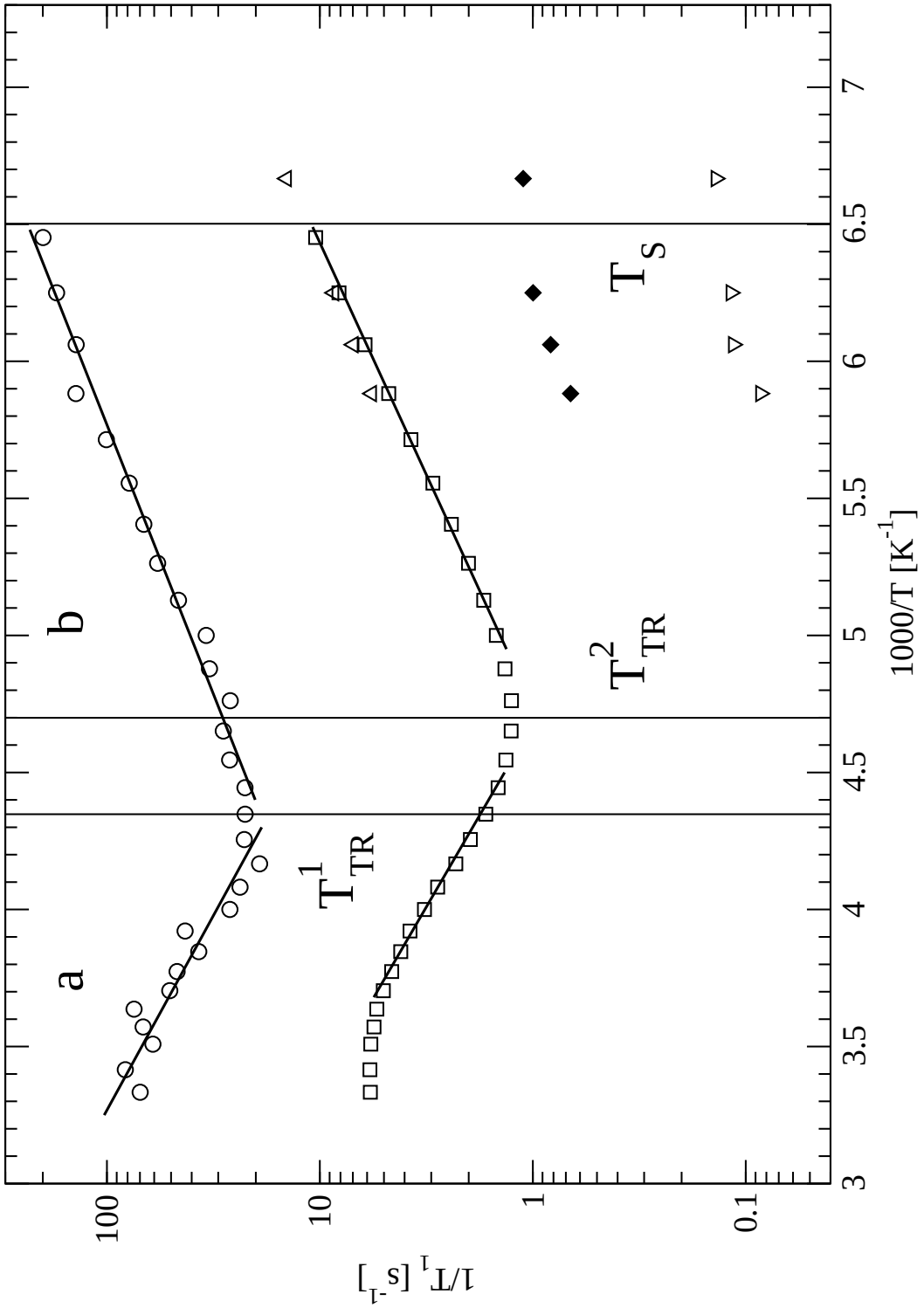

Fig. 5.

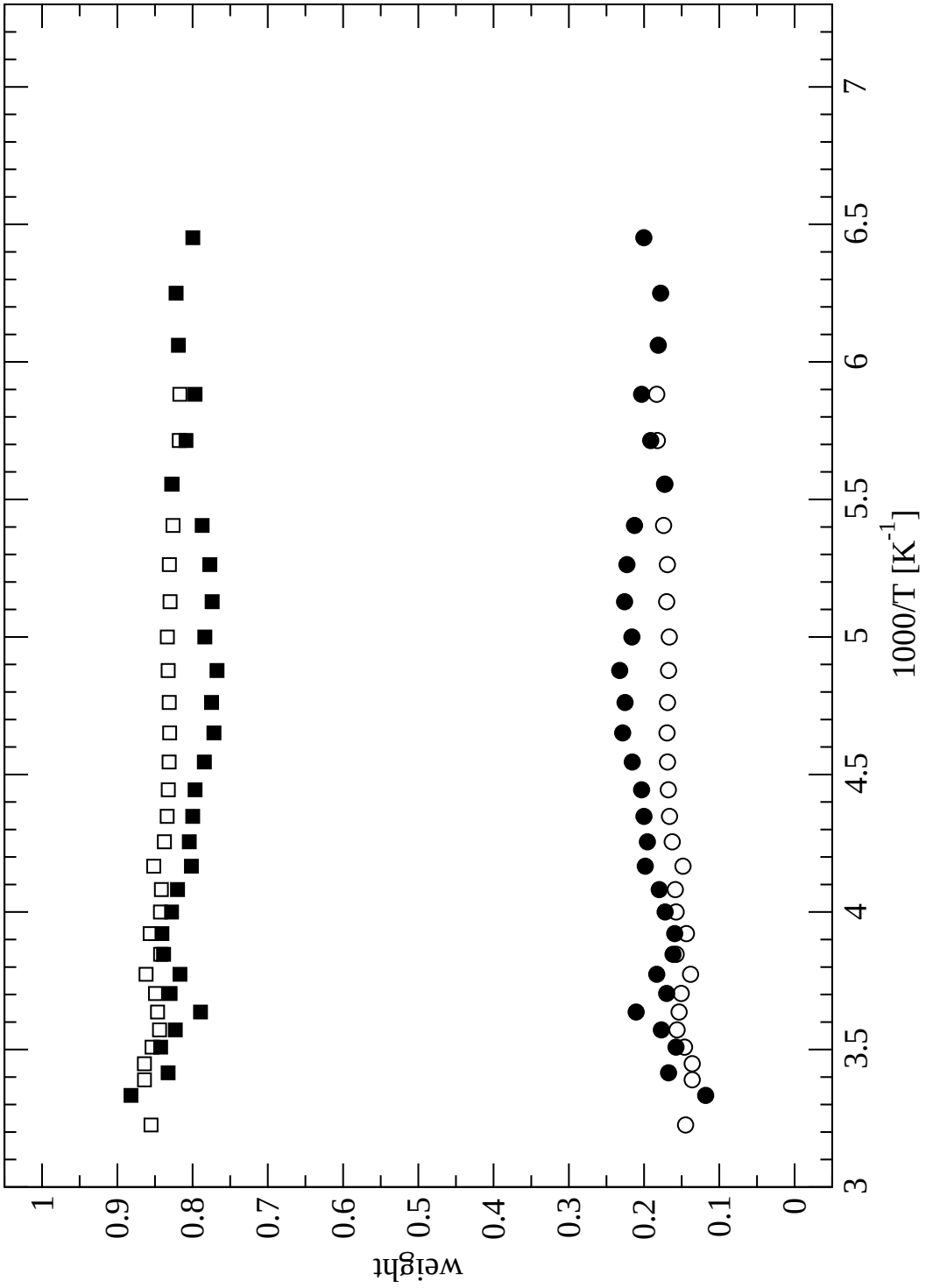

Fig. 6.

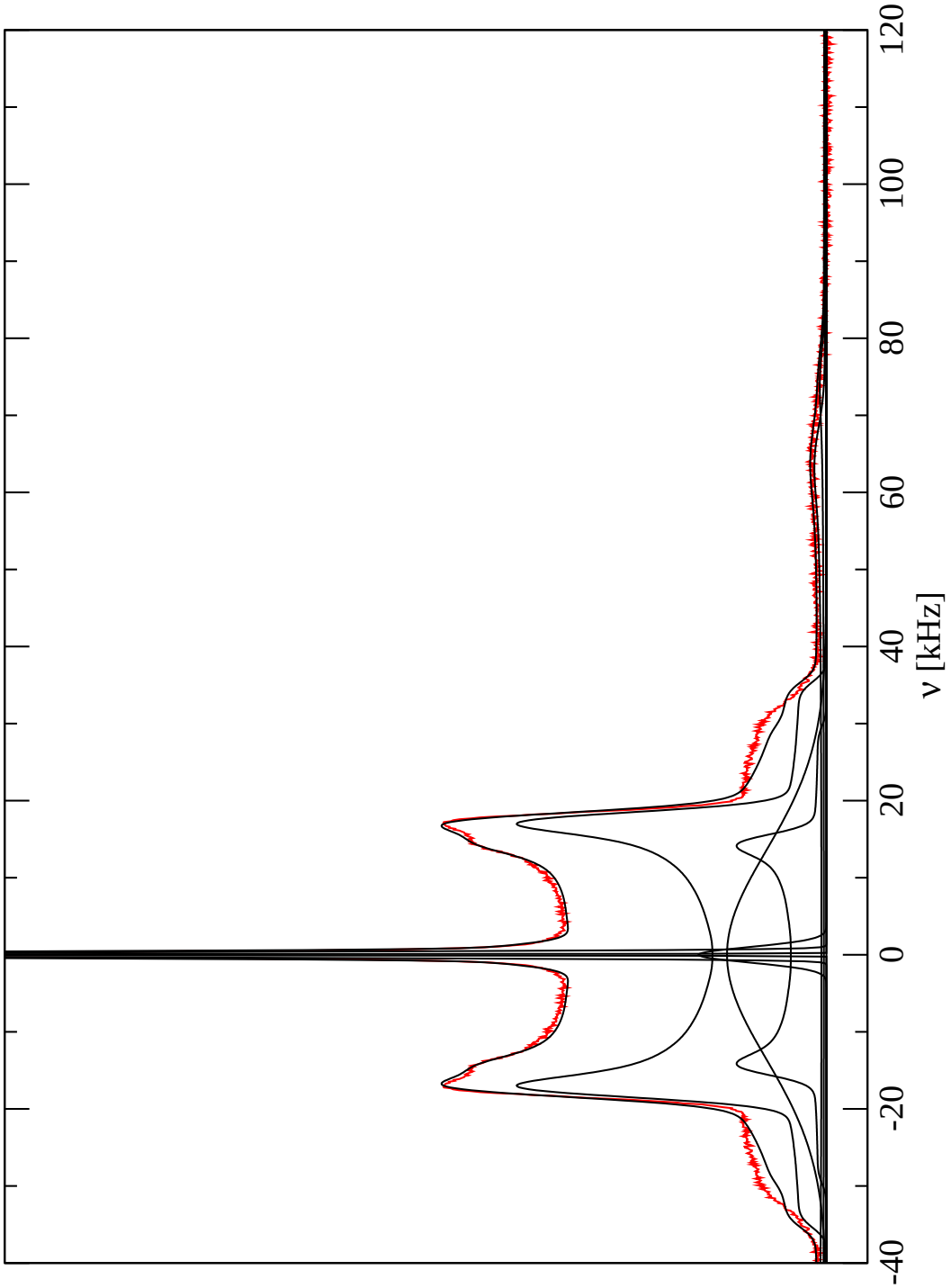

Fig. 7.

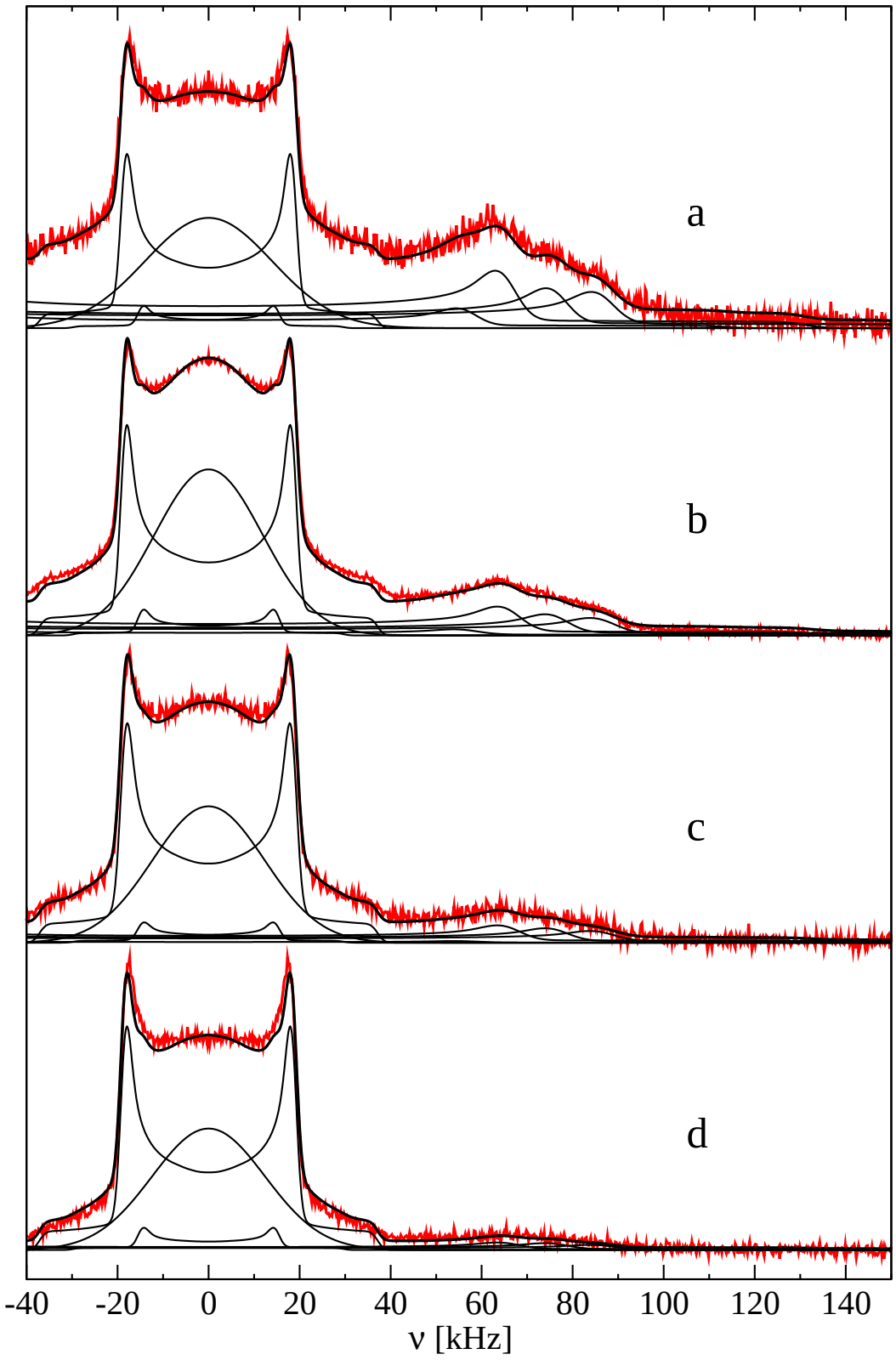

Fig. 8.

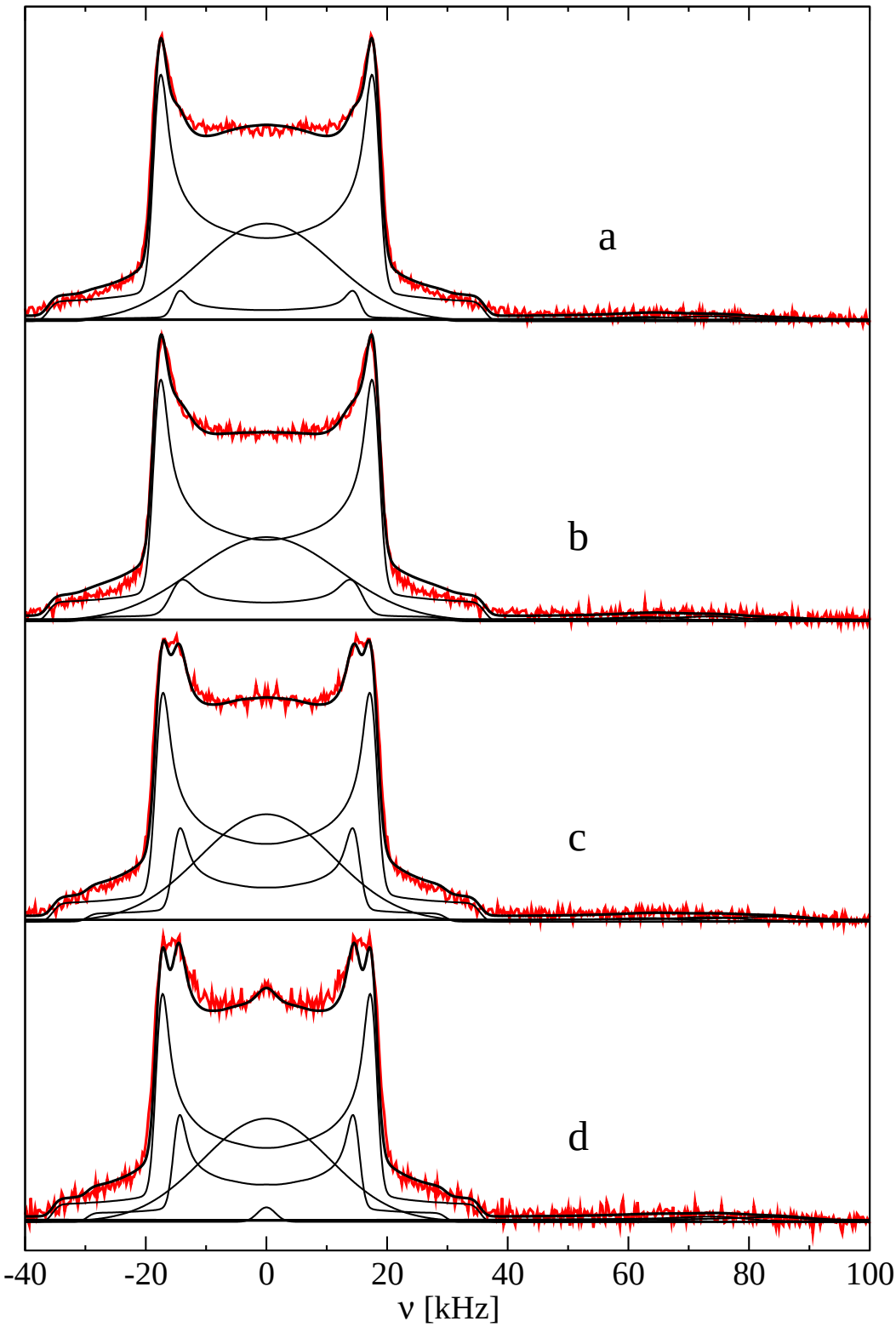

Fig. 9.

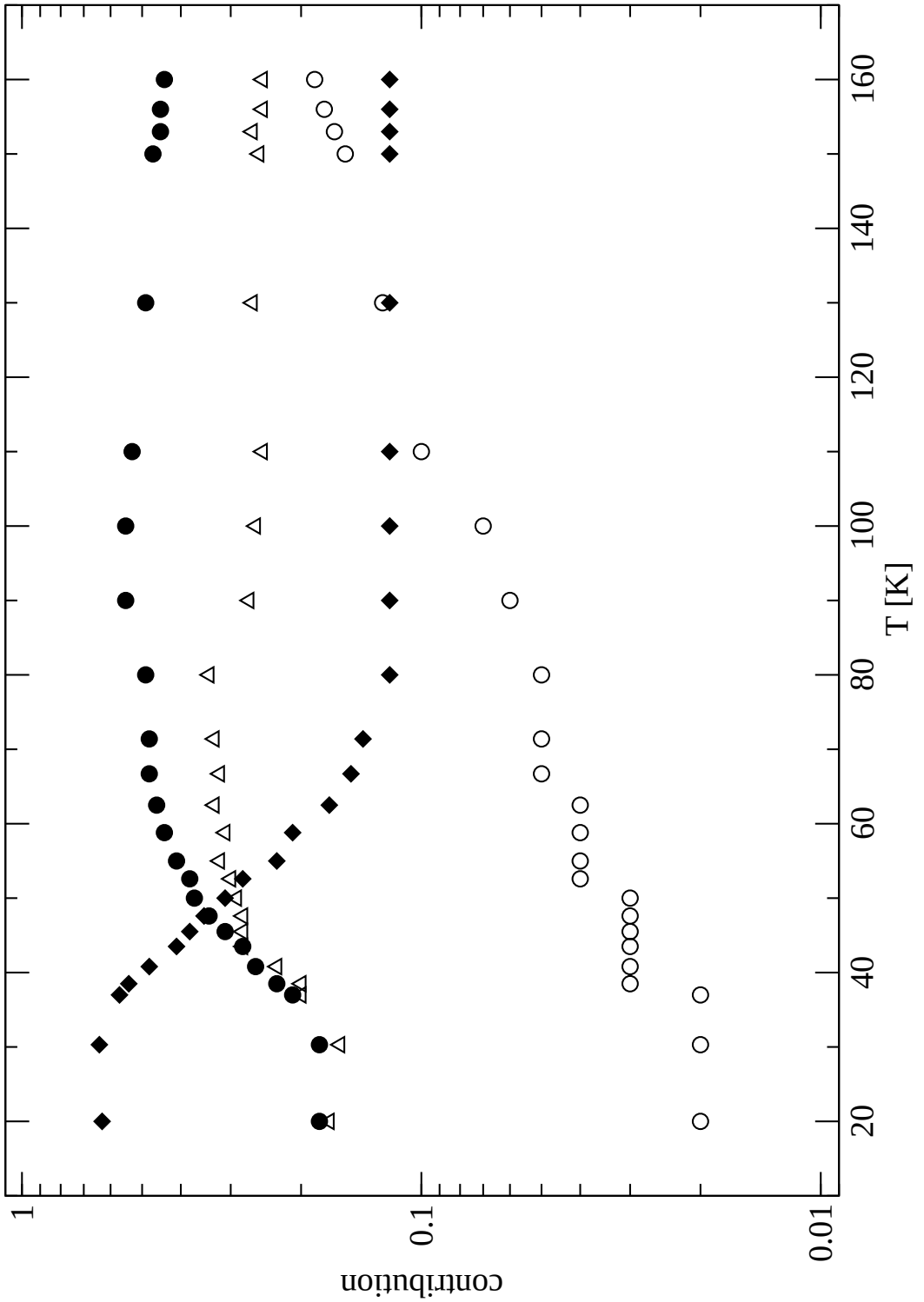

Fig. 10.

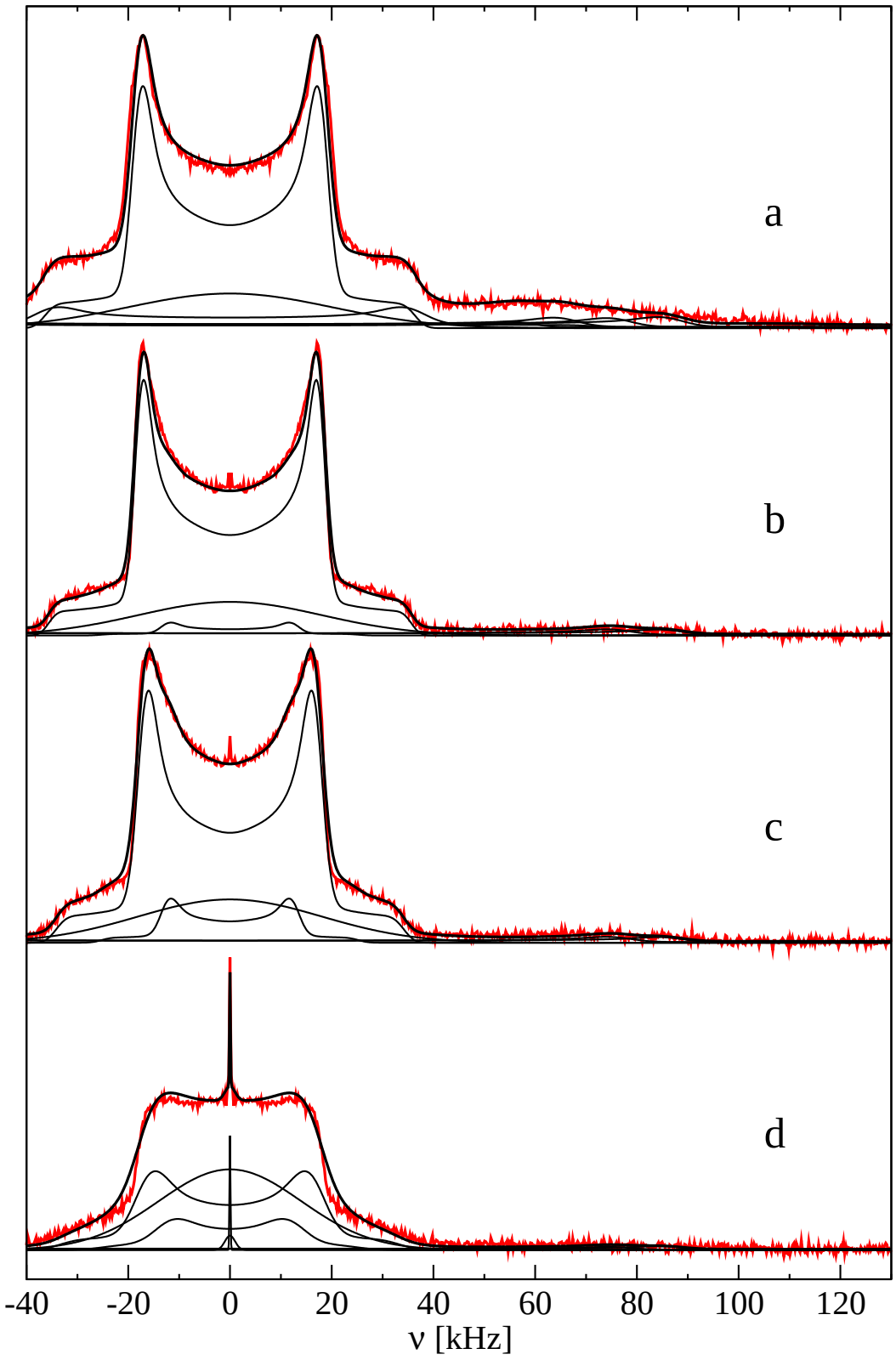

Fig. 11.

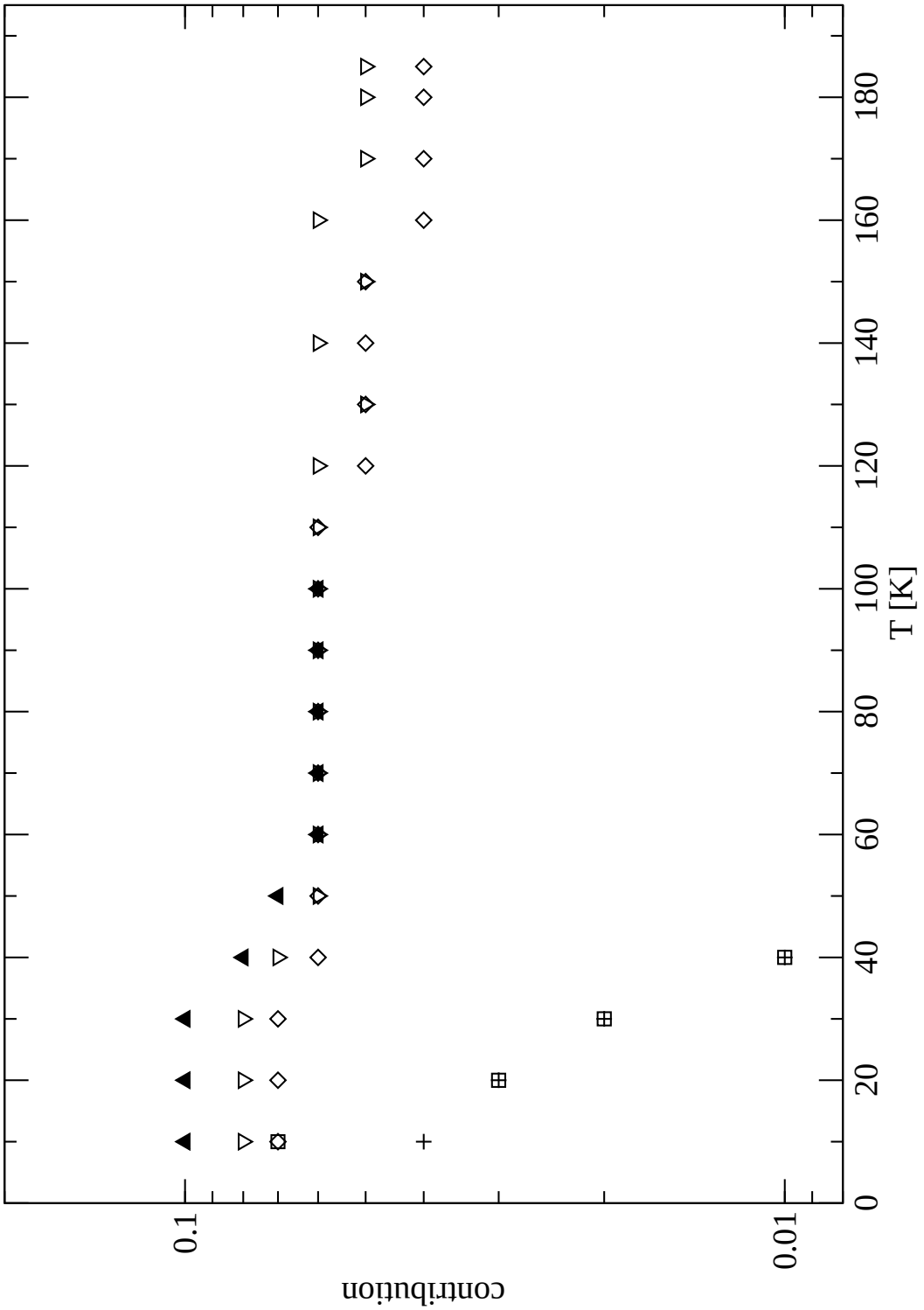

Fig. 12.

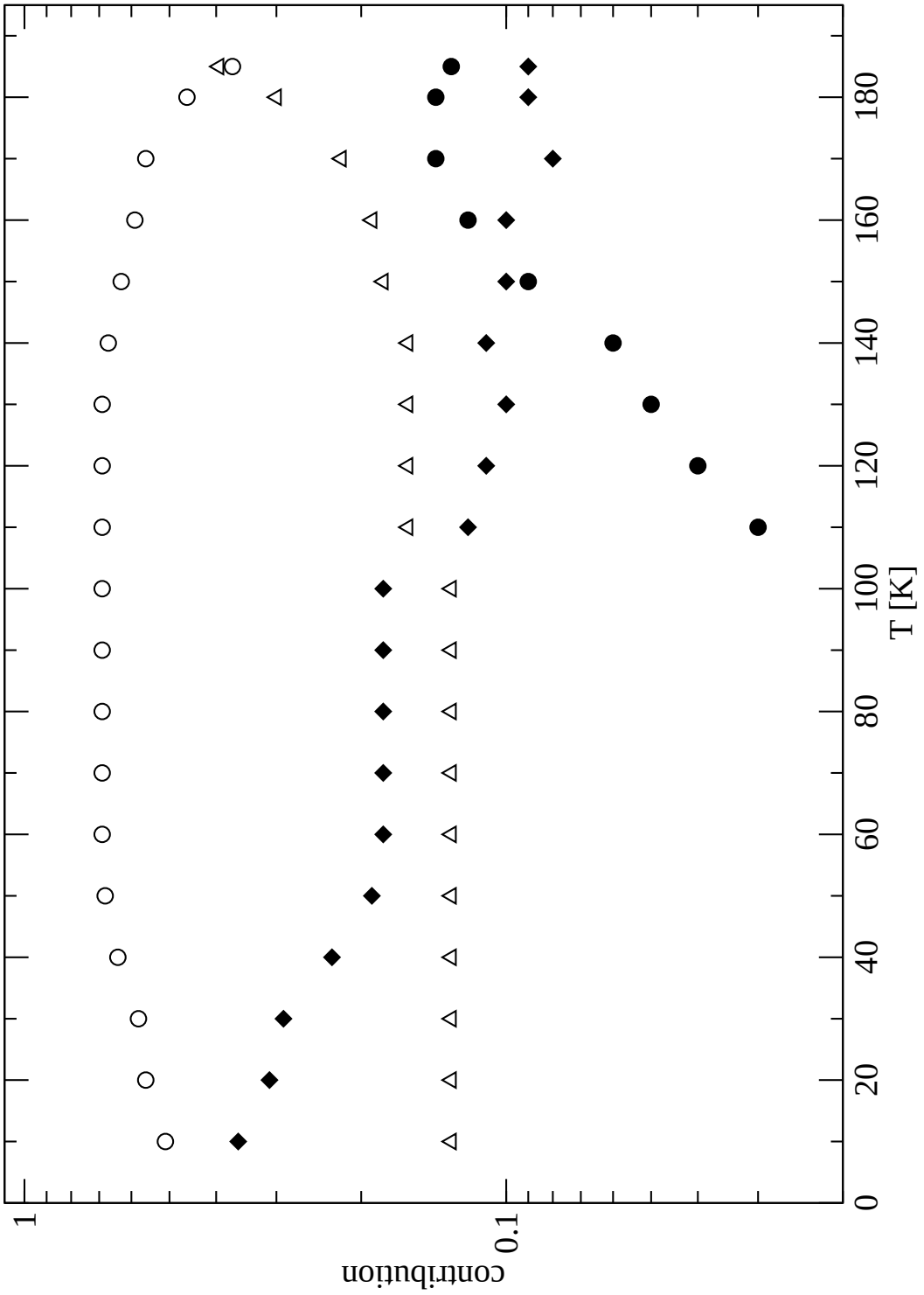

Fig. 13.

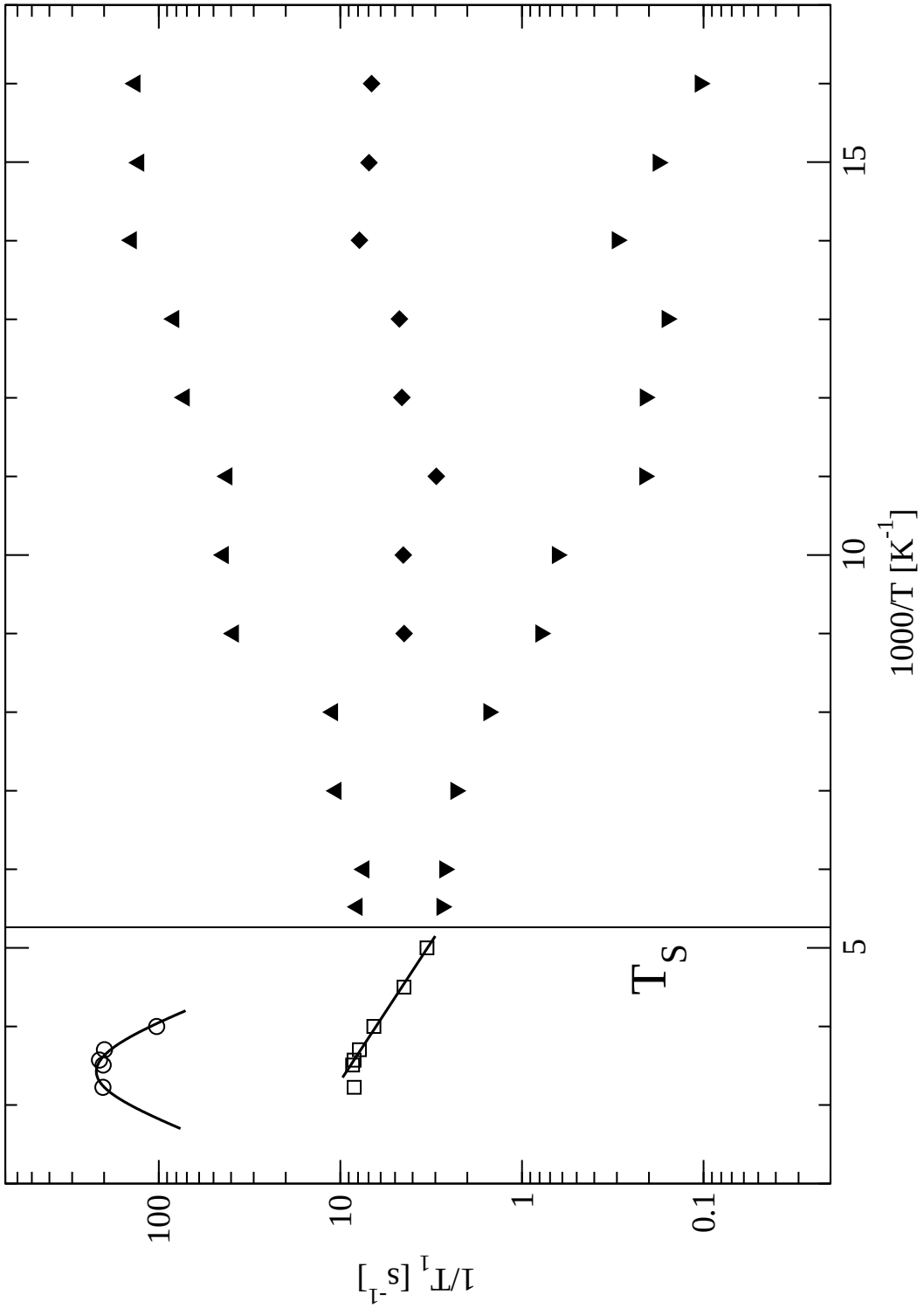

Fig. 14.